EPA Public Access
Author manuscript
Environ Sci Technol. Author manuscript; available in PMC 2022 December 07.
About author manuscripts | Submit a manuscript

Published in final edited form as:
Environ Sci Technol. 2021 December 07; 55(23): 15950–15960. doi:10.1021/acs.est.1c06067.

Plumbojarosite Remediation of Soil Affects Lead Speciation and Elemental Interactions in Soil and in Mice Tissues

Tyler D Sowers[1], **Sharon E Bone**[2], **Matthew R Noerpel**[3], **Matthew D Blackmon**[1], **Ranju R Karna**[4], **Kirk G Scheckel**[3], **Albert L Juhasz**[5], **Gary L Diamond**[6], **David J Thomas**[7], **Karen D Bradham**[1]

[1]Center of Environmental Measurement and Modeling, Office of Research and Development, US Environmental Protection Agency, Research Triangle Park, North Carolina 27711, United States.

[2]Stanford Synchrotron Radiation Lightsource, SLAC National Accelerator Laboratory, Menlo Park, California 94025, United States.

[3]Center for Environmental Solutions & Emergency Response, Office of Research and Development, US Environmental Protection Agency, Cincinnati, Ohio 45268, United States.

[4]Bennett Aerospace, Inc., Engineer Research and Development Center, USACE, Vicksburg, Mississippi 39183, United States.

[5]Future Industries Institute, University of South Australia, Mawson Lakes Campus, Adelaide, SA 5095, Australia.

[6]SRC, Inc., North Syracuse, New York 13212, United States.

[7]Center for Computational Toxicology & Exposure, Office of Research and Development, US Environmental Protection Agency, Research Triangle Park, North Carolina 27711, United States.

Abstract

Lead (Pb) contamination of soils is of global concern due to the devastating impacts of Pb exposure in children. Because early-life exposure to Pb has long-lasting health effects, reducing exposure in children is a critical public health goal that has intensified research on the conversion of soil Pb to low bioavailability phases. Recently, plumbojarosite (PLJ) conversion of highly available soil Pb was found to decrease Pb relative bioavailability (RBA <10%). However, there is sparse information concerning interactions between Pb and other elements when contaminated soil, pre- and post-remediation, is ingested and moves through the gastrointestinal tract (GIT). Addressing this may inform drivers of effective chemical remediation strategies. Here, we utilize bulk and micro-focused Pb X-ray absorption spectroscopy to probe elemental interactions and Pb speciation in mouse diet, cecum, and feces samples following ingestion of contaminated soils pre- and post-PLJ treatment. RBA of treated soils was less than 1% with PLJ phases transiting the GIT with little absorption. In contrast, Pb associated with organics was predominantly found in the cecum. These results are consistent with transit of insoluble PLJ to feces following ingestion.

Supporting Information
Pb XANES spectra and standards used for LCF; supplementary XRF mapping data for mouse model samples; and additional information on mouse model methodology (PDF)

The authors declare no competing financial interest.

EPA Author Manuscript
EPA Author Manuscript
EPA Author Manuscript

EPA Author Manuscript

EPA Author Manuscript

EPA Author Manuscript

The expanded understanding of Pb interactions during GIT transit complements our knowledge of elemental interactions with Pb that occur at higher levels of biological organization.

Keywords

PLJ; RBA; XANES; gastrointestinal tract; lead bioavailability; speciation; μ-XRF

Introduction

For children, ingestion of lead (Pb)-contaminated soil can be a significant source of exposure that promotes long-lasting adverse health effects. (1) Exposure during childhood is of particular concern because early-life Pb exposure interferes with brain development. (1–3) Early-life exposure to Pb is substantial. In the United States, elevated blood Pb levels (>5 μg Pb dL^{-1}) are found in at least 2.5% of children; (3) worldwide, blood Pb levels in as many as 800 million children exceed this standard. (4) Development of methods to assess and mitigate Pb exposure is an important area of research with *in vivo* models providing a reliable means to assess exposure to bioavailable Pb following ingestion of contaminated soil. (5–9) Oral bioavailability (absolute bioavailability; ABA) refers to the portion of the oral Pb dose that is absorbed from the gastrointestinal tract (GIT) into the systemic circulation. (5,10) Bioavailability of Pb in soil is often expressed in terms of relative bioavailability (RBA), which refers to the ratio of Pb ABA in soil to the ABA of a highly soluble reference form of Pb (e.g., lead acetate). (6,8)

In situ conversion of Pb in soils into less bioavailable forms may be a cost-effective strategy to reduce Pb exposure from contaminated soils. (5,11–13) These remediation strategies decrease soil Pb bioavailability by changing the physical and chemical properties of Pb present in soil. For example, phosphate amendment of Pb-contaminated soils has been shown to convert soluble Pb species in soil into less soluble and less bioavailable Pb-phosphate species. (11,14) A novel method for the remediation of Pb-contaminated soil involving the promotion of plumbojarosite (PLJ) precipitation has recently been identified as a remediation methodology with the potential to significantly reduce bioaccessibility and bioavailability compared to existing methodologies. (15) Plumbojarosite is a Pb-containing hydroxysulfate mineral—$Pb_{0.5}^{2+}Fe_3^{3+}(OH)_6(SO_4)_2$—that is highly stable under acidic pH (<4) conditions. (16–19) Slow addition of a ferric sulfate-0.01 M H_2SO_4 solution to a heated soil resulted in either complete or predominant (>90%) conversion of Pb species present to PLJ for all Pb standards and soils evaluated. (15) The bioavailability of the PLJ-treated soil has been assessed using a mouse model. The formation of PLJ markedly decreased RBA for Pb with RBA in treated soils <10%. (15) Although PLJ formation may be an efficient and cost-effective alternative to current methods for soil Pb remediation, additional studies are needed to extend the findings of recently published research and facilitate modification that allow for field application. For example, optimal conditions to promote PLJ in contaminated soils must be determined. Similarly, studies of the stability of Pb species formed in soil during treatment are needed to determine long-term persistence of the effects on soil lead bioavailability, facilitating the assessment of this novel method for soil Pb remediation.

EPA Author Manuscript EPA Author Manuscript EPA Author Manuscript

Chemical speciation of Pb is a critical determinant of its bioavailability. Speciation of ingested Pb is expected to change during transit through the GIT; (5,14) therefore, determination of Pb speciation changes is critical to assessing contaminant exposure. Two recent studies have paired X-ray fluorescence mapping and bioavailability assessments using samples collected after the inhalation or ingestion of Pb-contaminated dust or soils. (20,21) These studies highlighted Pb associations with iron (Fe) and calcium (Ca) pre- and post-phosphate treatment on the centimeter scale and found Pb concentrated in the stomach. In a dust inhalation study, X-ray absorption near-edge spectroscopy (XANES) found organically bound Pb to predominate in the small intestine; in lungs, Pb-phosphate complexes were predominant. (21) Differences in Pb speciation in different tissues presumably represent tissue-specific differences in the chemical environment (e.g., differences in pH and ionic composition) as well as biological processes that can affect Pb speciation. Hence, additional work is needed to connect bulk Pb speciation, spatially resolved elemental associations, and microscale speciation of the GIT in ingested soil. This information will help elucidate the relation between Pb speciation changes produced by soil remediation and changes in Pb absorption across the GIT barrier. To address the significant gaps in our understanding of changes in Pb speciation during GIT transit, (4,20) we used paired bulk and micro-XAS/XRF analyses to assess Pb speciation and elemental associations in samples representative of different steps in the exposure pathway associated with ingestion of Pb-contaminated soil. The pre-ingestion sample consisted of the diet into which the test soil was incorporated; the ingested sample consisted of the contents of the cecum, a component of the GIT located at the junction of the small and large intestine of the mouse; and the post-ingestion sample consisted of feces collected from mice that consumed the test soil-amended diet during the bioavailability assay.

In the work reported here, we examined changes in Pb bioavailability and speciation using two soils from Broken Hill, a large Pb–Zn–Ag mining site in New South Wales, Australia. Widespread contamination of soil and dust with Pb is well documented for this site and has been associated with high blood Pb levels in children residing near the mining site. (22–24) Analyses were performed using untreated soils and soils treated by a novel method that promotes PLJ formation. This investigation provides a window into soil Pb elemental interactions for a progression of the GIT, illustrating for the first time the chemistry of Pb bioavailability remediation technologies at the microscale.

Materials and Methods

Preparation of Soils

Surface soil samples (0–5 cm; $n = 12$) were collected from Broken Hill, New South Wales, Australia in 10 L plastic buckets along a south-east transect away from the line of lode. Following characterization (see Table S1), two soils (BHK5 and BHK10) were selected for bioavailability and spectroscopic analyses. Soils collected from Broken Hill were sieved to <250 μm and treated using the optimized plumbojarosite precipitation method developed for soils as described in Karna et al. (15) Treatment conditions included the slow addition (6 mL h^{-1}) of 120 mL of 0.1 M $Fe^{3+}(SO_4)$–0.01 M H_2SO_4 pumped to 1 L of soil suspension containing 20 g BHK soils. Reactions took place in a well-stirred 2 L reaction vessel

EPA Author Manuscript

EPA Author Manuscript

EPA Author Manuscript

at 95–100 °C for ~20 h. After the treatment was completed, the soils were isolated via centrifugation and washed three times with Milli-Q water (>18 MΩ). The washed residues were frozen at −20 °C, freeze-dried, and stored in a desiccator. Elemental concentrations for soils were determined via digestion (USEPA Method 3051) (25) and subsequent ICP-OES analysis (Table S1).

Mouse Model Bioavailability

Relative bioavailability of Pb in untreated or treated soils was determined using a previously described mouse model. (6) Test materials (untreated or treated soils or lead acetate, a highly soluble reference compound) were incorporated by a vendor (Dyets, Inc., Bethlehem, PA) into powdered AIN-93G rodent diet to prepare test diets. After a 12-day acclimation period, 6-week old female C57BL/6 mice (Charles River Laboratories; Raleigh, NC) were transferred to metabolic cages (Lab Products, Seaford, DE). During the 9-day assay, three mice in each metabolic cage had free access to test diet and drinking water. Consumption of diet was determined daily and cumulative diet intake was used to calculate the ingested dose of Pb. A cumulative feces sample was prepared for each metabolic cage by pooling of each day's feces. On the morning of day 9, the mice were euthanized by CO_2 anesthesia and exsanguination. After removal of skin and viscera, carcasses were de-fleshed by dermestid beetles to provide a complete skeleton for determination of the concentration of Pb in bone. Cumulative feces samples and the skeletons from each cage were homogenized using a model 6850 freezer mill (Spex, Metuchen, NJ) to prepare samples for analysis. Because the cage was the unit of analysis for these assays, each metabolic cage yielded a skeletal sample and a cumulative feces sample. Total elemental concentration of mouse model samples (Table S2) were determined via hotblock digestion (EPA Method 3050B) (26) followed by analysis of Pb using inductively coupled plasma-mass spectrometry (ICP-MS). Additional detail may be found in the Supporting Information.

Calculation of Relative Bioavailability

The bone-dose ratio method was used to calculate Pb RBA for all TMs (eq 1). This method uses data on Pb levels in bone and the amount of Pb consumed from test diets that contain a test material (untreated or treated soil) or Pb acetate, a highly soluble reference material.

$$\mathrm{RBA} = \frac{\mathrm{Bone}_{\mathrm{TM}}}{\mathrm{Dose}_{\mathrm{TM}}} / \frac{\mathrm{Bone}_{\mathrm{PbOAC}}}{\mathrm{Dose}_{\mathrm{PbOAc}}} \quad (1)$$

Here, $\mathrm{Bone}_{\mathrm{TM}}$ and $\mathrm{Bone}_{\mathrm{PbOAc}}$ are the background-corrected Pb concentrations in the total bone mass of mice fed diet amended with the test material or lead acetate, respectively, and $\mathrm{Dose}_{\mathrm{TM}}$ and $\mathrm{Dose}_{\mathrm{PbOAc}}$ are the respective cumulative ingested Pb doses. Rationale for and evaluation of the bone-dose ratio methodology are provided in Sowers et al. (27)

Lead X-ray Absorption Spectroscopy

Mouse diet, cecal contents, and feces were investigated using bulk L_{III}-edge Pb X-ray absorption spectroscopy. Spectra were collected using the Advance Photon Source (Argonne National Laboratory; Lemont, Chicago) at beamline 5BM-D (DuPont-Northwestern-Dow

EPA Author Manuscript EPA Author Manuscript EPA Author Manuscript

111 Collaborative Access Team). (28) Approximately 60 mg of sample was mixed with ~20 mg of poly(vinylpyrrolidone) and made into a 13 mm pellet using a benchtop pellet press (International Crystal Laboratories). Pellets were then surrounded with a single layer of Kapton tape on each side. The Kapton-taped sample pellet was then mounted at the Sector 5BM-D beamline and prepared for fluorescence measurement. Fluorescence detection was accomplished using two Vortex ME-4 four-element silicon drift detectors. The detectors were both oriented perpendicular to the beam on either side on the sample pellet which was placed at a 45° angle to the incidence beam. A Pb foil reference standard was mounted in front on the reference ionization chamber, allowing for simultaneous sample and reference spectra collection per scan. Incidence, transmission, and reference ionization chambers were all purged with pure nitrogen gas. The beamline was prepared for Pb L_3 edge fluorescence measurements by scanning incident X-ray energy using a cryogenically cooled silicon (Si) double-crystal (111) monochromator. All samples were scanned from 12 835 to 13 415 eV using a step scan technique.

Collected XAS data were then calibrated to the Pb reference foil, averaged, merged, background subtracted, and normalized using the Demeter software package. (29,30) Reference spectra were collected from a Pb reference foil concurrently with sample Pb fluorescence data and calibrated to 13 035 eV. Reference calibrated sample scans were then averaged for each sample, followed by background subtraction and post-edge normalization using the Athena program of the Demeter software package. (30) After XAS data processing was completed, we performed linear combination fitting (LCF) to identify Pb phases present in mouse model samples. LCF was performed in Athena (30) for the first derivative of the Pb X-ray absorption near-edge spectroscopy region for first-derivative Pb LCF from 13 010 to 13 100 eV. (29) A library of 24 Pb XAS standards were used to probe potential components present in each sample (Table S3). Standards were sequentially removed based on the statistical improvement of fit. Components contributing less than 10% were removed, followed by refitting with remaining components. The combination of standards resulting in the lowest *R*-factor results, signifying the statistically best fit for the data, for each sample was reported. It is important to note that spectra presented as Pb-adsorbed to Fe or Pb-adsorbed to clay may refer to a variety of Fe or clay phases, as specific phases within these groupings are challenging to identify using Pb XANES. All spectra concluded to be a significant LCF component are presented in Table S3.

μ-X-ray Fluorescence Mapping and Spatially Resolved Pb Speciation Analysis

Aliquots of the dried, ground samples were set in 1 mm thick epoxy disks and imaged via micro-X-ray fluorescence (μ-XRF) elemental mapping at beamline 10–2 at the Stanford Synchrotron Radiation Lightsource (SSRL). Sample maps were collected at 13 500 eV using a Si(111) $\phi = 90$ double-crystal monochromator with 25 μm resolution. The monochromator was calibrated by setting the maximum of the first derivative of a Pb foil to 13 035.0 eV. The fluorescent signal was monitored using a four-element solid-state Vortex Si-drift detector, which is an energy-dispersive detector that enables monitoring of multiple fluorescent lines, including those for Pb, Fe, Ca, and P. Pb K-edge μ-XANES were collected on selected locations, which were chosen based on the Pb concentration, and whether Pb was associated with any of the other elements monitored. Each spectrum comes from a 25 ×25 μm^2-area

EPA Author Manuscript

EPA Author Manuscript

EPA Author Manuscript

with a step size of 0.5 eV from 13 010 to 13 090 eV. All data processing was performed in Sam's Microanalysis ToolKit (SMAK). (31) The images presented herein were re-imaged in SMAK using a Gaussian blur function at 80% standard deviation to reduce image noise.

Results and Discussion

Effects of Soil Treatment on Pb Bioavailability

Two soils from the Broken Hill site designated BHK5 and BHK10 were evaluated with the mouse model. The RBAs for Pb in untreated BHK5 and BHK10 were 38.6 and 42.1%, respectively (Table 1). Treatment of soils to promote the formation of PLJ markedly reduced the Pb RBA. For either treated soil, the Pb RBA was <1%. Reduced Pb bioavailability of both treated BHK soils was consistent with recent work that found treatment to promote PLJ formation decreased Pb bioavailability in another set of test soils. (15) Notably, results of the current study and earlier work cited here show that the formation of PLJ significantly decreases Pb bioavailability. (15) By contrast, remediation of soils with phosphate had much more modest effects on Pb bioavailability in the mouse model. (5,11) These findings suggested that PLJ formation may be a superior method for remediation of Pb-contaminated soils, if scalable to field applications.

Identification of Pb Phases in Diet, Cecal Contents, and Feces

Speciation of Pb was examined in diet, cecal contents, and feces samples collected from mice that consumed the diet amended with either untreated or treated BHK soils or from mice that consumed diet amended with Pb acetate, a highly soluble Pb compound that is often used as the reference compound in assays that measure the RBA for Pb in animal models. This approach provided information on changes in Pb speciation that occurred during transit of the GIT as well as differences in speciation found in two soils treated to promote PLJ formation.

Pb X-ray absorption near-edge spectroscopic data and overlaid linear combination fits (LCFs) are shown in Figure 1, with LCF results demonstrating relative contributions of different Pb species to the diet, cecal contents, and feces obtained from mice that consumed untreated or treated BHK soils (Figure 2 and Tables S4 and S5). Bulk Pb XANES analyses revealed that Pb speciation changed during GIT transit. In untreated BHK5 diet, Pb adsorbed to hydroxyapatite (HAP) predominated with contributions of Pb adsorbed to Fe (oxyhydr)oxide and Pb citrate. Pb citrate may serve as a proxy for Pb associated with carboxylic moieties in organic matter present in soil or diet. The absence of Pb citrate in cecal contents or feces collected from these mice suggested that phosphate interactions between HAP and Pb had higher stabilities than Pb adsorbed to goethite or associated with carboxylic-rich organic matter. Treatment of BHK5 soil affected Pb speciation in diet. The absence of Pb adsorbed to HAP in diet likely reflected the highly acidic, near-boiling (95–100 °C) conditions used for PLJ treatment, (15,32) which converted most of HAP-associated Pb to PLJ. In cecal contents from mice that consumed diet with treated BHK10 soil, Pb citrate and Pb cysteine accounted for all Pb present. As noted above, Pb citrate is thought to represent interactions between carboxyl moieties and Pb. Pb cysteine may be a proxy for interactions between Pb and cysteinyl residues present in peptides and proteins. (33) In

EPA Author Manuscript EPA Author Manuscript EPA Author Manuscript

contrast to differences for Pb speciation in diet and cecal contents, the profile of Pb species found in feces resembled that found in diet. PLJ was not found in the cecal contents, which is likely explained by complete transition of PLJ phases from the GIT and released via feces. It is unlikely that organic-associated Pb phases are derived from PLJ due to the high stability in acidic conditions and low bioavailability of PLJ. Rather, Pb in the cecum is expected to have been released from sorbed Pb phases, which will be discussed further.

Diet, cecal contents, and feces from mice that consumed diets amended with untreated and treated BHK10 soil were also evaluated via Pb XANES speciation analysis. Diet amended with untreated BHK10 soil contained Pb adsorbed to bentonite or to goethite and pyromorphite. These findings indicated that the soil used for diet preparation contained heterogeneous Pb-solid phases in which interactions with clay are expected to greatly influence the Pb chemistry present. Pb speciation was also affected by the presence of Fe(III) (oxyhydr)oxides and phosphate minerals present in this soil. Pb speciation in cecal contents from mice that consumed diet amended with untreated BHK10 soil contained goethite but was dominated by Pb associated with carboxylic moieties and cysteine. By comparison, Pb adsorbed to clay/Fe (oxyhydr)oxide and pyromorphite accounted for Pb found in feces from mice that consumed diet amended with untreated BHK10 soil. Specific adsorbed phases are challenging to specifically identify using Pb XANES; therefore, specific clay and Fe (oxyhydr)oxide phases are not concluded to facilitate Pb adsorption. Treatment of BHK10 soil to promote PLJ formation produced changes in Pb speciation that resembled those found in treated BHK5 soil. PLJ was the dominant Pb species in both the diet consumed by and feces collected from mice that consumed treated BHK10 soil. In contrast to findings with treated BHK5 soil, cecal contents from mice consuming treated BHK10 soil contained PLJ as well as Pb adsorbed to Fe (oxyhydr)oxide and Pb cysteine.

These Pb speciation data from studies using untreated or treated soils provide insights into factors that may influence Pb bioavailability. For both untreated and treated soils, there was good concordance between relative amounts of different Pb species found in diet and feces. That is, for both untreated and treated soils, the most abundant Pb species in diet and feces were the same. In contrast, the profiles for Pb species in cecal contents were not reliably predicted by the profiles of species found in diet or feces. For both untreated soils, Pb species in cecal contents showed marked changes from those found in diet. These included loss of an organic Pb species (Pb citrate) in cecal contents from mice that consumed untreated BHK5 soil and the appearance of Pb citrate and Pb cysteine in cecal contents from mice that consumed untreated BHK10 soil. Notably, PLJ was absent from cecal contents of mice that consumed diets amended with treated BHK5 soil; only organic Pb species were found in these samples. Similarly, cecal contents from mice that consumed diet amended with treated BHK10 soil did not contain PLJ as a predominant component (28 ± 1.5%). It is not expected that PLJ phases are dissolving in this system as gastric pH (3–4) and cecal content pH (~5.7–6) should not significantly influence PLJ solubility. (34,35) Additionally, RBA was exceptionally low for both treated BHK5 and BHK10; therefore, the lack of PLJ in the cecal contents is expected to be due to movement out of the cecal contents and into the feces, The appearance of organic Pb species in cecal contents may reflect the release of Pb adsorbed to Fe (oxyhydr)oxide under acidic conditions (pH ~3) occurring in the upper GIT (5,6,36) Negatively charged organic components of the cecum derived from the

EPA Author Manuscript

EPA Author Manuscript

EPA Author Manuscript

microflora of this tissue and its contents derived from ingested diet and from intestinal secretions may readily bind desorbed cationic Pb(II). (37,38) Investigations probing Pb complexation with biologically common thiols and cysteine in solution have shown that Pb may readily complex with proteins and enzymes; (39,40) therefore, soluble Pb may readily interact with organic constituents of cecal contents. Similarly, organic-associated Pb has been found in a previous XAS analysis of the contents of the small intestine of mice exposed to Pb-contaminated house dust, (21) providing further support that organic-associated Pb play a role in altering Pb speciation during GIT transit. While organic-associated Pb species were found to be important components in the cecal contents for all samples, PLJ-treated samples are expected to have remained stable throughout the GIT due to low solubility, strong resistance to acidity, predominant PLJ concentration in the feces, and exceptionally low RBA for both treated soils (<1%).

Organic-associated Pb in the cecal contents of those receiving treated soils are expected to be predominantly, if not entirely, sourced from Pb sorbed phases that are present in the diet. For BHK5 and BHK10 treated soils, differing Pb speciation in mouse diet, cecal contents, and feces may be partly explained by the rapid transport of highly stable and poorly soluble PLJ through the GIT. The contribution of organic Pb species found in cecal contents to the amount of Pb that is bioavailable is not well understood. In mice, there are at least two pathways for Pb absorption across the GIT barrier, including transport mediated by the divalent metal transporter 1 (DMT1) and transport by another transporter that is functionally distinct from DMT1. (41) Expression of DMT1 and presumably capacity for Pb transport varies across the mouse GIT with the highest expression found in the duodenum. DMT1 is also expressed in the epithelia of mouse cecum, (42) suggesting that soluble organic Pb species found in this tissue could contribute to Pb uptake. The relative importance of DMT1-dependent and -independent Pb uptake to the bioavailability of Pb in soil remains unquantified as does the extent of Pb species by these pathways. PLJ phases likely limit Pb availability for transportation via DMT1, resulting in PLJ phase concentration in the feces. Soluble Pb components are likely expressed to the greatest extent in the cecal contents due to interactions with the DMT1 protein.

Visualization of Changes in Pb Speciation during GIT Transit

Species identified using bulk Pb XAS analyses were connected to spatially resolved spectrometric analyses to probe the chemical environment that affects Pb speciation across the GIT (Figures 3–5, S1, and S2). These analyses focused on diet, cecal contents, and feces from mice that consumed diet amended with treated BHK soil. Elemental micro-X-ray fluorescence (μ-XRF) RGB maps overlaying Pb (green), Fe (red), and Ca (blue) were developed for these samples (Figure 3). Combinations of these elemental signatures provided insight into elemental associations that occurred in diet containing treated BHK5 soil (Figures 3a and S3–S6). Here, a relatively large particle shaded yellow in this sample reflected similar XRF contributions of Pb (green) and Fe (red) to its composition and may be a large particle of Pb-containing soil that was integrated into the diet. Evidence of Pb and Fe interactions found in bulk Pb XAS results for diet amended with treated BHK5 soil (Figure 2) were consistent with the results shown in Figure 3a and suggested that particles consisted mostly of Fe-rich PLJ ($Pb_{0.5}^{2+}Fe_3^{3+}(OH)_6(SO_4)_2$) with a minor fraction of Pb-adsorbed

EPA Author Manuscript

EPA Author Manuscript

EPA Author Manuscript

goethite. Notably, Pb hot spot areas that were not congruent with spectral evidence of elemental interactions with Fe may reflect the presence of Pb that was unassociated with PLJ phases. In cecal contents (Figure 3b), Pb-containing particles were smaller and less apparent than in diet. There were a few areas indicative of Pb–Fe interactions (yellow); however, these areas were not predominant. Minimal Pb elemental interactions in cecal contents likely reflect the dominance of Pb-C interactions that were not detected by μ-XRF analysis. Feces from mice that consumed diet amended with treated BHK5 soil (Figure 3c) was found to contain Fe-rich particles (red) with many possessing signatures of Pb. Traces of Pb were clearly present and associated with Fe when evaluating the map in the absence of Fe detection (Figure 4d); however, Fe fluorescence was significantly elevated compared to Pb, resulting in most particles present being primarily red-shaded. Visually, Fe appeared to concentrate in feces as the strong signal for particulate Fe was absent from the diet. As noted earlier, bulk XAS indicated that Pb in diet and feces was present primarily as PLJ and Pb adsorbed goethite.

A separate analysis evaluated the phosphorous occurrence and distribution in diet consumed by and feces collected from mice that consumed a diet amended with treated BHK5 soil (Figure 4). Here, interactions of Pb, Fe, and P in diet with treated BHK5 soil were signaled by the presence of a dominantly white particle; its color reflected similar contributions of all three elements to its composition (Figure 4a). Additionally, this particle—along with smaller, unassociated particles—had vibrant Pb signatures (Figure 4b). In feces, particles had stronger signatures for both P and Fe (i.e., purple) than for Pb (Figure 4c,d). The predominance of the P and Fe signals may be driven by the accumulation of phosphates and Fe in the contents of the GIT. The relative strengths of the P, Fe, and Pb signals suggested that high P–Fe particles were important vessels for Pb. Bulk Pb XANES analysis found that about 90% of Pb in feces was present as PLJ. This suggested that Fe-rich particles in feces were likely PLJ with P either adsorbed to and/or partially substituted for sulfate in the PLJ mineral structure. (43,44) Notably, AIN-93G rodent diet which was the basal diet used for these assays contained on a weight basis 0.3% P with approximately equal amounts of P contributed by potassium phosphate and by phosphoproteins in casein, the diet's protein source. (45) Thus, sufficient levels of soluble P were provided from diet to account for the interactions between this element and Pb.

All GIT phases evaluated were found to contain spatially unique elemental associations. These findings suggested, although PLJ remained stable during GIT transit, its particle size and elemental co-associations may change in response to changes in the levels of other elements which can interact with PLJ. The absence of PLJ in cecal contents from mice that consumed diet amended with treated BHK5 soil suggested that XAS analysis could provide insights into interactions among elements in cecal contents. μ-XRF images of cecal contents from mice that consumed diets amended with pre- and post-treatment BHK5 soil or with Pb acetate found that Pb–Fe interactions were not common in cecal contents from any treatment group (Figure 5). There are few comparable data on Pb mapping in tissues, although there are limited data on Pb speciation by centimeter-scale XRF analysis of tissues from mice following intratracheal instillation of Pb-contaminated soils. (20,21) Findings from the present study affirmed this earlier work indicating that Pb–Fe interactions are not prevalent. However, our work did detect Pb–Fe microparticles in cecal contents that could

EPA Author Manuscript

EPA Author Manuscript

EPA Author Manuscript

not be detected in earlier studies that used less sensitive instrumentation for Pb detection. Therefore, the results of the present study provide novel insights into soil Pb interactions at a scale of analysis previously unattainable.

Spatially Resolved μ-XAS Analysis of Metal Interactions in Cecal Contents

μ-XRF analysis of diet, cecal contents, and feces indicated that interactions between Pb and other elements changed during transit of the GIT. This finding prompted the use of μ-XANES to probe Pb speciation of representative microaggregates found in cecal contents (Figures 5 and S8 and Table S6). Although the cecum is a unique structural modification found in the mouse GIT, (46) interactions between Pb and other elements that occur in cecal contents can be taken as a surrogate for interactions that occur at other sites for Pb absorption in the GIT. Furthermore, the complex microbiota of the mouse cecum may result in changes in Pb speciation that are mediated by microorganisms present in this tissue. (47,48)

For these analyses, we examined elemental interactions in cecal contents from mice that consumed diets amended with untreated BHK5 soil or with treated BHK5 soil. For comparison, we also examined interactions among elements in cecal contents from mice that consumed diet amended with Pb acetate, a soluble Pb species used in mouse assays as a reference compound. Elemental composition was determined using first-derivative LCF analysis in two Pb hotspots in XRF maps for each cecal content (Figure 5a–c).

Composition of cecal contents from mice that consumed diet amended with untreated BHK5 determined by μ-XANES were similar to those found in bulk Pb XANES results. Here, region S1 rich in Fe and Pb (i.e., yellow) consisted predominantly of Pb-adsorbed to Fe(III) oxide with a small contribution from Pb adsorbed to hydroxyapatite (Table S6). The significant presence of Fe-associated Pb was consistent with μ-XRF results showing a strong co-association between Pb and Fe in cecal contents. The presence of both Pb phases was reasonable given that both phases were found in the bulk Pb XANES LCF; however, bulk analysis found Pb adsorbed to hydroxyapatite to be the predominant phase. Region S2 was found to be 100% Pb adsorbed to hydroxyapatite, reflecting the bulk Pb XANES LCF results and XRF results comparing Pb, Fe, and P in this sample (Figure S8). XRF revealed the S2 particle was dominantly Pb (i.e., green) (Figure 4a), indicating that Fe was not extensively associated with Pb in this particle and supports its identity as Pb adsorbed to hydroxyapatite. The μ-XANES analysis of the cecal contents from mice consuming diet containing untreated BHK5 soil showed that Fe-rich particles can persist at the microscale. Fe (oxyhydr)oxide-associated Pb may have different bioavailability from Pb associated with hydroxyapatite, emphasizing the importance of accounting for micron-level biogeochemical processes that may mediate contaminant bioavailability.

Speciation of Pb in cecal contents from mice that consumed diet amended with treated BHK5 soil was examined using paired μ-XRF and XANES analysis. Regions S3 and S4 were chosen based on substantial Pb and Fe signatures found in this sample (Figure 5b). Although bulk XANES analyses did not identify PLJ in cecal contents, this Pb species was found by μ-XRF to account for most of the Pb. S3 contained about 96% PLJ along with a minor contribution from anglesite (4%). In S4, PLJ accounted for about 52% of the Pb

EPA Author Manuscript

EPA Author Manuscript

EPA Author Manuscript

with the remainder contributed by Pb adsorbed to Fe(III) oxide. Although carbon was not detectable at the energy range analyzed for the XRF mapping samples, the bulk Pb XANES data indicated that organic-associated Pb species were present in the cecal contents. As previously discussed, the finding of organic-associated Pb in the cecum was consistent with the results of another study that found organic-associated Pb in the mouse small intestine. (21) The detection of PLJ particles by μ-XANES/XRF analysis suggested that, although a small fraction of this Pb species was retained in the cecal contents, most of the PLJ transited the GIT quickly. The overall Pb speciation of the cecal contents is still expected to be PLJ as identified by the bulk analyses, but PLJ microsites do exist as revealed by the μ-XANES. The low solubility of PLJ through the GIT is consistent with other findings (15) and accounted for the detection of PLJ alone in feces from mice that consumed diet amended with treated BHK5 soil.

Pb speciation by elemental mapping and μ-XANES in cecal contents of mice that consumed diet amended with Pb acetate provided insights into the role of soil in the formation and fate of Pb species in the GIT (Figure 5c). Pb was widely distributed in cecal contents from mice exposed to Pb acetate with no clear relation between the distributions of Pb and other elements (Fe, Ca, etc.). μ-XANES analysis of two regions S5 and S6 identified Pb acetate as the only Pb species present, suggesting that Pb acetate was fully solubilized and available for transport across the GIT barrier. This finding of high solubility supports the continued use of Pb acetate as an appropriate reference compound for use in assays that assess the bioaccessibility and/or bioavailability of Pb in soils and other matrices.

Significance of Paired Spatial and Bulk XAS Investigations for Pb Bioavailability

To our knowledge, this is the first report in which bulk Pb XANES LCF analysis and spatially resolved XANES analysis were paired to examine changes in Pb speciation in soils during transit of the GIT. These findings were consistent with other work showing that Pb speciation may change following inhalation or consumption. (5,21) We found that treatment of two highly contaminated soils from Broken Hill, Australia complex efficiently promoted PLJ formation and decreased the RBA for Pb to <1%. The reduction of RBA in treated soils was associated with changes in Pb speciation that were characterized by an array of spectroscopic and spectrometric methods. Application of these techniques showed that PLJ in treated soils was excreted in feces, which is consistent with the reduction in RBA resulting from low solubility of PLJ in the GIT. The expanded understanding of elemental–Pb interactions occurring across the GIT complements our knowledge of interactions between elements (e.g., Fe, Ca, P) and Pb that occur at higher levels of biological organization. For example, although changes in Fe, Ca, or P nutrition have long been known to affect uptake of Pb across the GIT and to affect tissue distribution and retention of Pb at the whole animal level, (49) elemental interactions that may contribute to these effects are not completely understood. Studies of Pb speciation as material transits the GIT provide a new tool to determine the basis of interactions between essential nutrients and Pb. This knowledge may help refine methods for soil remediation to favor the formation of highly insoluble Pb species with low bioavailability.

EPA Author Manuscript

EPA Author Manuscript

EPA Author Manuscript

The detection of organic-associated Pb species in cecal contents raises new questions about the origin and fate of these species. In particular, we do not have a clear understanding of the role of organic-associated Pb species in the transporter-mediated uptake of Pb across the GIT barrier. Citrate-Pb interactions related to absorption and transport have been observed. In mice, supplementation of the diet with citrate has been shown to increase the bioavailability of lead acetate. (50) Erythrocyte ghosts take up Pb when exposed to a Pb-citrate buffer, and Pb transfer across the erythrocyte membrane appears to be linked to anion exchange. (51,52) Some aspects of formation of organic-associated Pb species may be addressed in future studies that pair bulk and spatially resolved C speciation analysis. Similarly, the study of the transporter-mediated uptake of organic Pb complexes may be facilitated by the use of three-dimensional models of the epithelium of the GIT. Further exploration of the kinetics and chemistry of PLJ transport throughout the entire GIT is needed to acquire a better understanding of the lack of PLJ found in the bulk cecum and the role of PLJ microsites that may remain in the GIT. Likewise, PLJ-forming remediation methods represent a newly developed technology that will require further adaptation for future field application. We expect this treatment to work effectively for a variety of soils, as showcased in Karna et al., (15) but should be definitively assessed in future investigations.

Supplementary Material

Refer to Web version on PubMed Central for supplementary material.

Acknowledgments

Pb speciation analysis was performed at the DuPont-Northwestern-Dow Collaborative Access Team (DND-CAT) located at Sector 5 of the Advanced Photon Source (APS). DND-CAT is supported by Northwestern University, E.I. DuPont de Nemours & Co., and The Dow Chemical Company. This research used resources of the Advanced Photon Source, a U.S. Department of Energy (DOE) Office of Science User Facility operated for the DOE Office of Science by Argonne National Laboratory under Contract No. DE-AC02-06CH11357. Portions of this work were funded by U.S. Environmental Protection Agency Office of Superfund Remediation and Technology Innovation (OSRTI) under Contract 68HERH19D022 (Task Order 68HERH19F0313). This document is being subjected to review by the Center of Environmental Measurement and Modeling (CEMM) for publication. Approval does not signify that the contents reflect the views of the Agency, nor does mention of trade names or commercial products constitute endorsement or recommendation for use. Use of the Stanford Synchrotron Radiation Lightsource, SLAC National Accelerator Laboratory, is supported by the U.S. Department of Energy, Office of Science, Office of Basic Energy Sciences under Contract No. DE-AC02-76SF00515.

References

1. Zartarian V; Xue J; Tornero-Velez R; Brown J. Children’s lead exposure: A multimedia modeling analysis to guide public health decision-making. Environ. Health Perspect 2017, 125, 097009 DOI: 10.1289/EHP1605 [PubMed: 28934096]
2. Betts KS CDC Updates Guidelines for Children’s Lead Exposure; National Institute of Environmental Health Sciences, 2012.
3. A Low Level Lead Exposure Harms Children: A Renewed Call of Primary Prevention; CDC: Atlanta, GA, 2012.
4. Rees N; Fuller R. The Toxic Truth: Children’s Exposure to Lead Pollution Undermines a Generation of Future Potential; UNICEF, 2020.
5. Bradham KD; Diamond GL; Nelson CM; Noerpel M; Scheckel KG; Elek B; Chaney RL; Ma Q; Thomas DJ Long-term in situ reduction in soil lead bioavailability measured in a mouse model. Environ. Sci. Technol 2018, 52, 13908–13913, DOI: 10.1021/acs.est.8b04684 [PubMed: 30358995]

EPA Author Manuscript EPA Author Manuscript EPA Author Manuscript

6. Bradham KD; Green W; Hayes H; Nelson C; Alava P; Misenheimer J; Diamond GL; Thayer WC; Thomas DJ Estimating relative bioavailability of soil lead in the mouse. J. Toxicol. Environ. Health, Part A 2016, 79, 1179–1182, DOI: 10.1080/15287394.2016.1221789
7. Bradham KD; Laird BD; Rasmussen PE; Schoof RA; Serda SM; Siciliano SD; Hughes MF Assessing the bioavailability and risk from metal-contaminated soils and dusts. Hum. Ecol. Risk Assess 2014, 20, 272–286, DOI: 10.1080/10807039.2013.802633
8. Casteel SW; Weis CP; Henningsen GM; Brattin WJ. Estimation of relative bioavailability of lead in soil and soil-like materials using young swine. Environ. Health Perspect 2006, 114, 1162–1171, DOI: 10.1289/ehp.8852 [PubMed: 16882520]
9. Ng JC; Juhasz A; Smith E; Naidu R. Assessing the bioavailability and bioaccessibility of metals and metalloids. Environ. Sci. Pollut. Res 2015, 22, 8802–8825, DOI: 10.1007/s11356-013-1820-9
10. Deshommes E; Tardif R; Edwards M; Sauvé S; Prévost M. Experimental determination of the oral bioavailability and bioaccessibility of lead particles. Chem. Cent. J 2012, 6, 138 DOI: 10.1186/1752-153X-6-138 [PubMed: 23173867]
11. Scheckel KG; Diamond L; Burgess MF; Klotzbach JM; Maddaloni M; Miller BW; Partridge CR; Serda SM Amending soils with phosphate as means to mitigate soil lead hazard: a critical review of the state of the science. J. Toxicol. Environ. Health, Part B 2013, 16, 337–380, DOI: 10.1080/10937404.2013.825216
12. Scheckel KG; Ryan JA Spectroscopic speciation and quantification of lead in phosphate-amended soils. J. Environ. Qual 2004, 33, 1288–1295, DOI: 10.2134/jeq2004.1288
13. Juhasz AL; Scheckel KG; Betts AR; Smith E. Predictive capabilities of in vitro assays for estimating Pb relative bioavailability in phosphate amended soils. Environ. Sci. Technol 2016, 50, 13086–13094, DOI: 10.1021/acs.est.6b04059 [PubMed: 27934280]
14. Bradham KD; Nelson CM; Diamond GL; Thayer WC; Scheckel KG; Noerpel M; Herbin-Davis K; Elek B; Thomas DJ Dietary Lead and Phosphate Interactions Affect Oral Bioavailability of Soil Lead in the Mouse. Environ. Sci. Technol 2019, 53, 12556–12564, DOI: 10.1021/acs.est.9b02803 [PubMed: 31557437]
15. Karna RR; Noerpel MR; Nelson C; Elek B; Herbin-Davis K; Diamond G; Bradham K; Thomas DJ; Scheckel KG Bioavailable soil Pb minimized by in situ transformation to plumbojarosite. Proc. Natl. Acad. Sci. U.S.A 2021, 118, e2020315117 DOI: 10.1073/pnas.2020315117 [PubMed: 33431689]
16. Baron D; Palmer CD Solubility of jarosite at 4–35 C. Geochim. Cosmochim. Acta 1996, 60, 185–195, DOI: 10.1016/0016-7037(95)00392-4
17. Dutrizac J; Kaiman S. Synthesis and properties of jarosite-type compounds. Can. Mineral 1976, 14, 151–158
18. Dutrizac JE; Jambor JL Jarosites and their application in hydrometallurgy. Rev. Mineral. Geochem 2000, 40, 405–452, DOI: 10.2138/rmg.2000.40.8
19. Forray FL; Smith AM; Drouet C; Navrotsky A; Wright K; Hudson-Edwards KA; Dubbin W. Synthesis, characterization and thermochemistry of a Pb-jarosite. Geochim. Cosmochim. Acta 2010, 74, 215–224, DOI: 10.1016/j.gca.2009.09.033
20. Kastury F; Smith E; Doelsch E; Lombi E; Donnelley M; Cmielewski PL; Parsons DW; Scheckel KG; Paterson D; De Jonge MDIn vitro, in vivo, and spectroscopic assessment of lead exposure reduction via ingestion and inhalation pathways using phosphate and iron amendments. Environ. Sci. Technol 2019, 53, 10329–10341, DOI: 10.1021/acs.est.9b02448 [PubMed: 31356748]
21. Kastury F; Smith E; Lombi E; Donnelley MW; Cmielewski PL; Parsons DW; Noerpel M; Scheckel KG; Kingston AM; Myers GRDynamics of lead bioavailability and speciation in indoor dust and x-ray spectroscopic investigation of the link between ingestion and inhalation pathways. Environ. Sci. Technol 2019, 53, 11486–11495, DOI: 10.1021/acs.est.9b03249 [PubMed: 31460750]
22. Dong C; Taylor MP; Gulson B. A 25-year record of childhood blood lead exposure and its relationship to environmental sources. Environ. Res 2020, 186, 109357 DOI: 10.1016/j.envres.2020.109357
23. Kristensen LJ; Taylor MP Unravelling a ‘miner’s myth’that environmental contamination in mining towns is naturally occurring. Environ. Geochem. Health 2016, 38, 1015–1027, DOI: 10.1007/s10653-016-9804-6 [PubMed: 26919836]

EPA Author Manuscript EPA Author Manuscript EPA Author Manuscript

24. Gulson BL; Howarthl D; Mizon KJ; Law AJ; Korsch MJ; Davis JJ Source of lead in humans from Broken Hill mining community. Environ. Geochem. Health 1994, 16, 19–25, DOI: 10.1007/BF00149589 [PubMed: 24198173]
25. US EPA. Method 3051. Microwave Assisted Acid Digestion of Sediments, Sludges, Soils, and Oils. SW-846 Method A, 1994.
26. US EPA. Method 3050B. Acid Digestion of Sediments, Sludges, and Soils. Revision 2. Test Methods for Evaluating Solid Wastes: Physical/Chemical Methods, EPA SW-846 Section A, 1996.
27. Sowers TD; Nelson CM; Diamond GL; Blackmon MD; Jerden ML; Kirby AM; Noerpel MR; Scheckel KG; Thomas DJ; Bradham KD High Lead Bioavailability of Indoor Dust Contaminated with Paint Lead Species. Environ. Sci. Technol 2021, 55, 402–411, DOI: 10.1021/acs.est.0c06908 [PubMed: 33307690]
28. Segre C; Leyarovska N; Chapman L; Lavender W; Plag P; King A; Kropf A; Bunker B; Kemner K; Dutta P. In The MRCAT Insertion Device Beamline at the Advanced Photon Source, AIP Conference Proceedings; American Institute of Physics, 2000; pp 419–422.
29. Kelly S; Hesterberg D; Ravel B. Analysis of Soils and Minerals Using X-Ray Absorption Spectroscopy. In Methods of Soil Analysis Part 5 – Mineralogical Methods; Soil Science Society of America: Madison, WI, 2008; Vol. 5, pp 387–463.
30. Ravel B; Newville M. ATHENA, ARTEMIS, HEPHAESTUS: data analysis for X-ray absorption spectroscopy using IFEFFIT. J. Synchrotron Radiat 2005, 12, 537–541, DOI: 10.1107/S0909049505012719 [PubMed: 15968136]
31. Webb S. In The MicroAnalysis Toolkit: X-Ray Fluorescence Image Processing Software, AIP Conference Proceedings; American Institute of Physics, 2011; pp 196–199.
32. Dutrizac J; Dinardo O; Kaiman S. Factors affecting lead jarosite formation. Hydrometallurgy 1980, 5, 305–324, DOI: 10.1016/0304-386X(80)90022–5
33. Farkas E; Buglyó P. Lead (II) Complexes of Amino Acids, Peptides, and Other Related Ligands of Biological Interest. In Lead: Its Effects on Environment and Health; De Gruyter, 2017; Vol. 17, p 201.
34. Fallingborg J. Intraluminal pH of the human gastrointestinal tract. Danish Med. Bull 1999, 46, 183–196 [PubMed: 10421978]
35. McConnell EL; Basit AW; Murdan S. Measurements of rat and mouse gastrointestinal pH, fluid and lymphoid tissue, and implications for in-vivo experiments. J. Pharm. Pharmacol 2010, 60, 63–70, DOI: 10.1211/jpp.60.1.0008
36. Sparks DL Environmental Soil Chemistry; Academic Press, 2003.
37. Gustafsson JP; Tiberg C; Edkymish A; Kleja DB Modelling lead (II) sorption to ferrihydrite and soil organic matter. Environ. Chem 2011, 8, 485–492, DOI: 10.1071/EN11025
38. Kaiser M; Ellerbrock R; Gerke H. Cation exchange capacity and composition of soluble soil organic matter fractions. Soil Sci. Soc. Am. J 2008, 72, 1278–1285, DOI: 10.2136/sssaj2007.0340
39. Mah V; Jalilehvand F. Lead (II) complex formation with glutathione. Inorg. Chem 2012, 51, 6285–6298, DOI: 10.1021/ic300496t [PubMed: 22594853]
40. Jalilehvand F; Sisombath NS; Schell AC; Facey GA Lead (II) complex formation with L-cysteine in aqueous solution. Inorg. Chem 2015, 54, 2160–2170, DOI: 10.1021/ic5025668 [PubMed: 25695880]
41. Elsenhans B; Janser H; Windisch W; Schümann K. Does lead use the intestinal absorptive pathways of iron? Impact of iron status on murine 210Pb and 59Fe absorption in duodenum and ileum in vivo. Toxicology 2011, 284, 7–11, DOI: 10.1016/j.tox.2011.03.005 [PubMed: 21397655]
42. Takeuchi K; Bjarnason I; Laftah AH; Latunde-Dada GO; Simpson RJ; McKie AT Expression of iron absorption genes in mouse large intestine. Scand. J. Gastroenterol 2005, 40, 169–177, DOI: 10.1080/00365520510011489 [PubMed: 15764147]
43. Aguilar-Carrillo J; Villalobos M; Pi-Puig T; Escobar-Quiroz I; Romero F. Synergistic arsenic (V) and lead (II) retention on synthetic jarosite. I. Simultaneous structural incorporation behaviour and mechanism. Environ. Sci.: Processes Impacts 2018, 20, 354–369, DOI: 10.1039/C7EM00426E
44. Dutrizac JE; Chen TT The behaviour of phosphate during jarosite precipitation. Hydrometallurgy 2010, 102, 55–65, DOI: 10.1016/j.hydromet.2010.02.004

EPA Author Manuscript

EPA Author Manuscript

EPA Author Manuscript

45. Reeves PG; Nielsen FH; Fahey GC Jr AIN-93 Purified Diets for Laboratory Rodents: Final Report of the American Institute of Nutrition Ad Hoc Writing Committee on the Reformulation of the AIN-76A Rodent Diet; Oxford University Press, 1993.
46. Hugenholtz F; de Vos WM Mouse models for human intestinal microbiota research: a critical evaluation. Cell. Mol. Life Sci 2018, 75, 149–160, DOI: 10.1007/s00018-017-2693-8 [PubMed: 29124307]
47. Zaborin A; Penalver Bernabe B; Keskey R; Sangwan N; Hyoju S; Gottel N; Gilbert JA; Zaborina O; Alverdy JC Spatial compartmentalization of the microbiome between the lumen and crypts is lost in the murine cecum following the process of surgery, including overnight fasting and exposure to antibiotics. mSystems 2020, 5, e00377–20 DOI: 10.1128/mSystems.00377-20 [PubMed: 32518197]
48. Kozik AJ; Nakatsu CH; Chun H; Jones-Hall YL Comparison of the fecal, cecal, and mucus microbiome in male and female mice after TNBS-induced colitis. PLoS One 2019, 14, e0225079 DOI: 10.1371/journal.pone.0225079 [PubMed: 31703107]
49. Dongre RSLead: Toxicological Profile, Pollution Aspects and Remedial Solutions; InTechOpen, 2020.
50. Spickett J;Bell R;Stawell J;Polan SThe influence of dietary citrate on the absorption and retention of orally ingested lead. Agents Actions 1984, 15, 459–462, DOI: 10.1007/BF01972388 [PubMed: 6524532]
51. Simons T. Influence of lead ions on cation permeability in human red cell ghosts. J. Membr. Biol 1985, 84, 61–71, DOI: 10.1007/BF01871648 [PubMed: 3999125]
52. Simons T. The role of anion transport in the passive movement of lead across the human red cell membrane. J. Physiol 1986, 378, 287–312, DOI: 10.1113/jphysiol.1986.sp016220 [PubMed: 3025431]

EPA Author Manuscript

EPA Author Manuscript

EPA Author Manuscript

Synopsis

Plumbojarosite treatment of lead-contaminated soils effectively decreases bioavailability, whereas lead associated with organic phases persists in the body.

EPA Author Manuscript

EPA Author Manuscript

EPA Author Manuscript

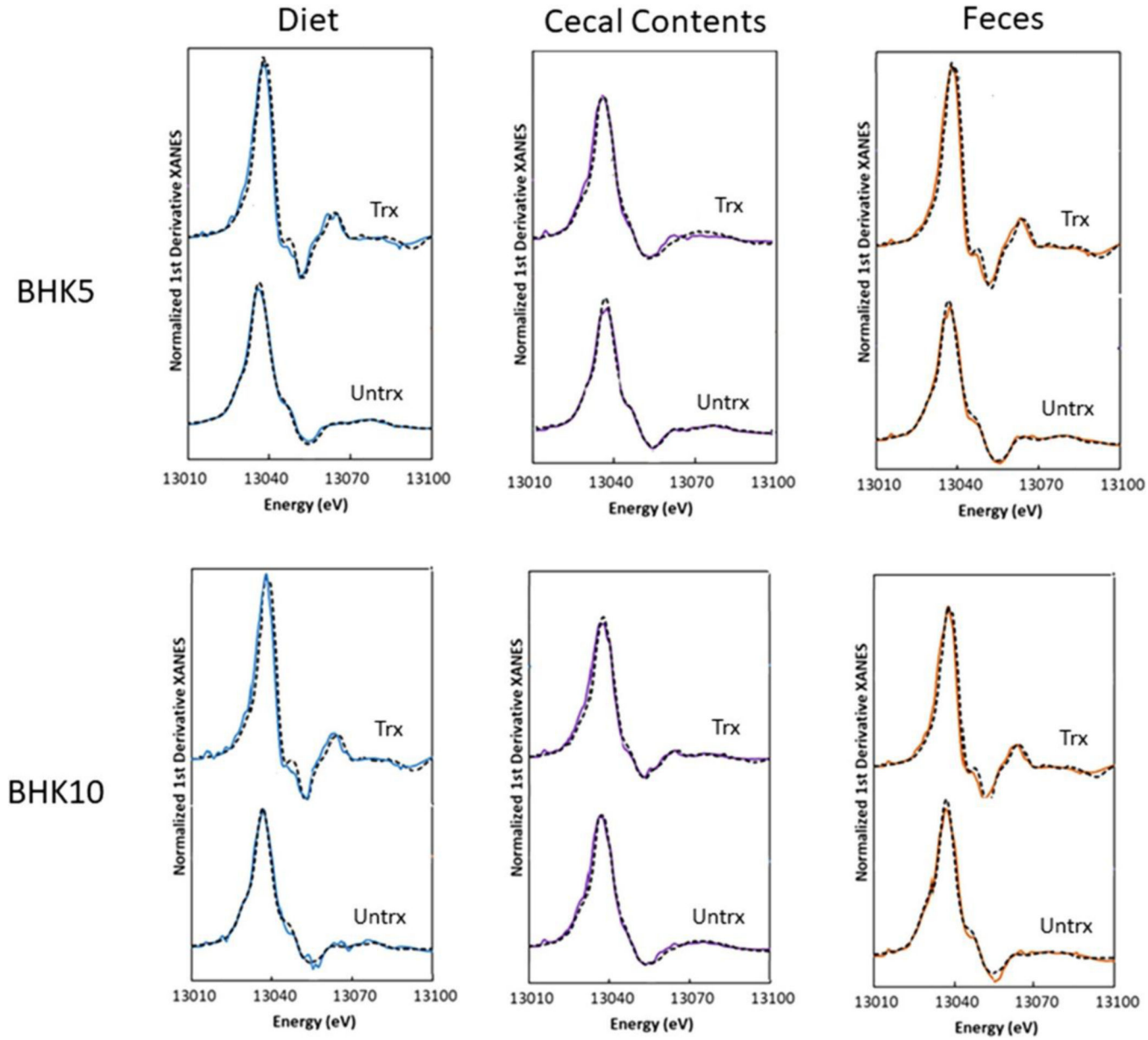

Figure 1.

Pb X-ray absorption near-edge spectroscopic data (solid lines) and linear combination fits (dashed lines) for untreated (Untrx) or treated (Trx) BHK5 and BHK10 soils.

EPA Author Manuscript

EPA Author Manuscript

EPA Author Manuscript

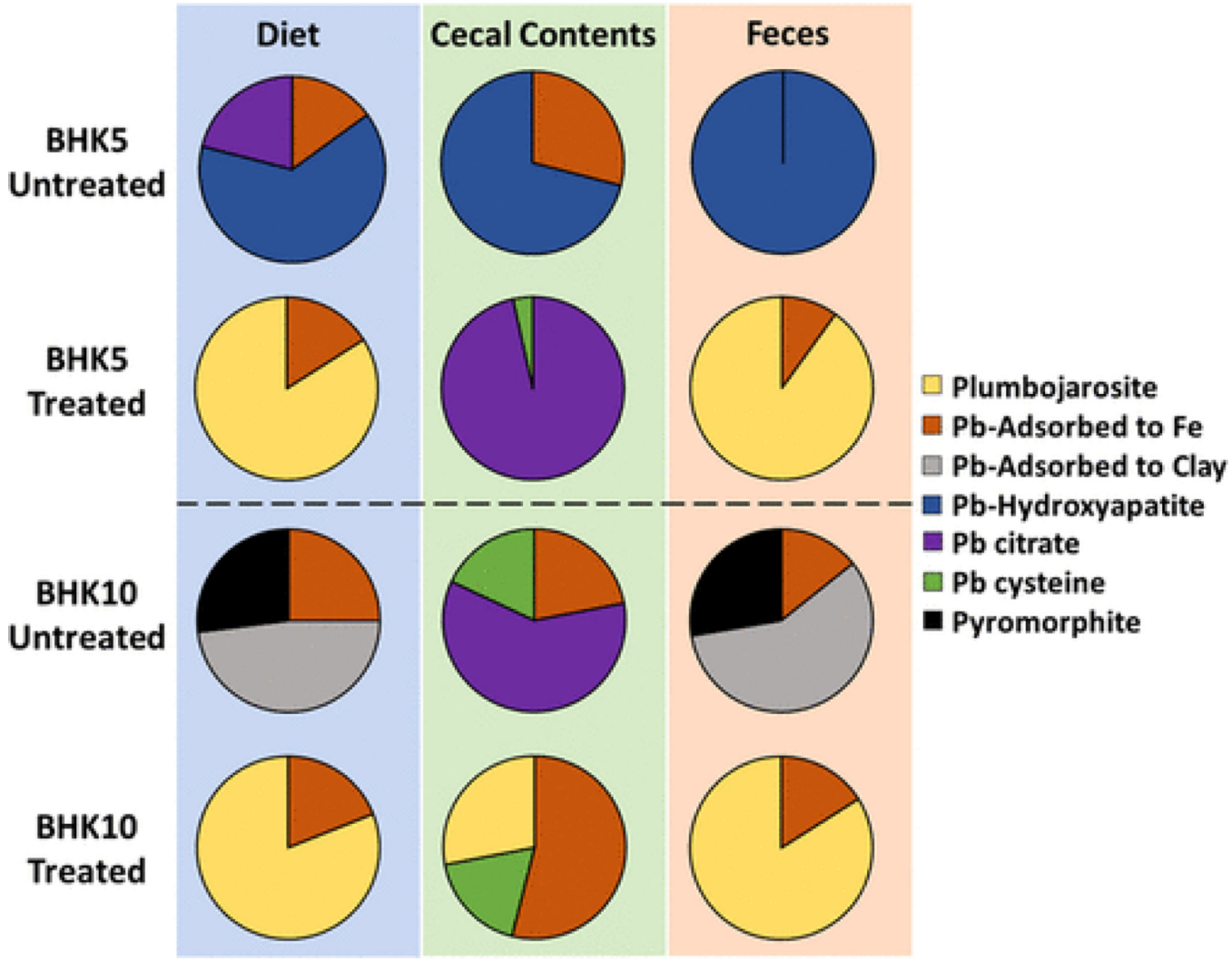

Figure 2.

Relative contribution of Pb species in consumed diet, cecal contents, and feces collected from mice that ingested diets amended with untreated or treated BHK5 or BHK10 soil. “Pb-Adsorbed to Fe” and “Pb-Adsorbed to Clay” are representative of spectra for Pb adsorbed to goethite and Pb adsorbed to bentonite, respectively. Quantitative LCF results are tabulated in the Supporting Information (Tables S3 and S4), including LCF results for diet, cecal content, and feces following Pb acetate ingestion.

EPA Author Manuscript

EPA Author Manuscript

EPA Author Manuscript

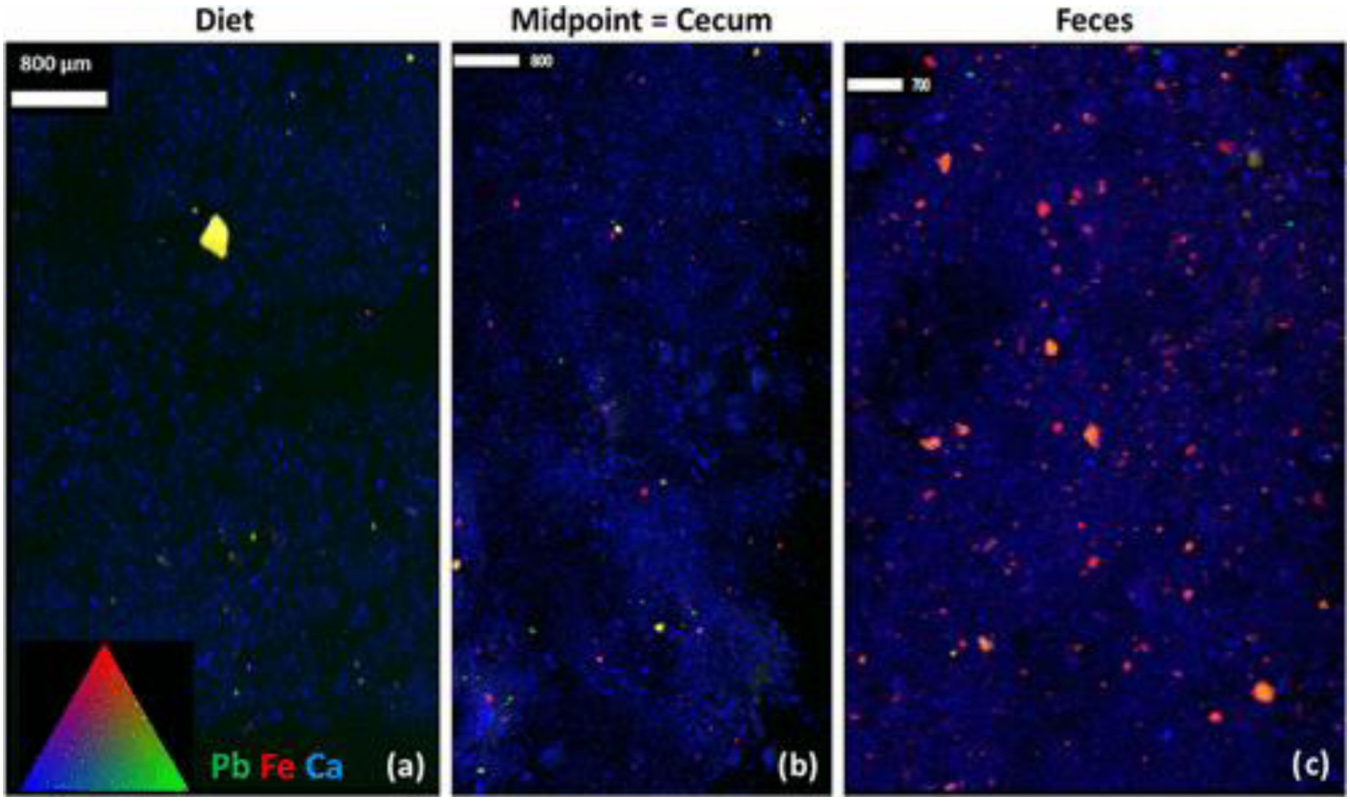

Figure 3.

µ-XRF mapping data for the (a) diet, (b) cecum, and (c) feces of a mouse that was fed BHK5-treated soil (2-D, 2-C, and 2-F, respectively, SI Figure S4). Scale bar is in micrometers.

EPA Author Manuscript

EPA Author Manuscript

EPA Author Manuscript

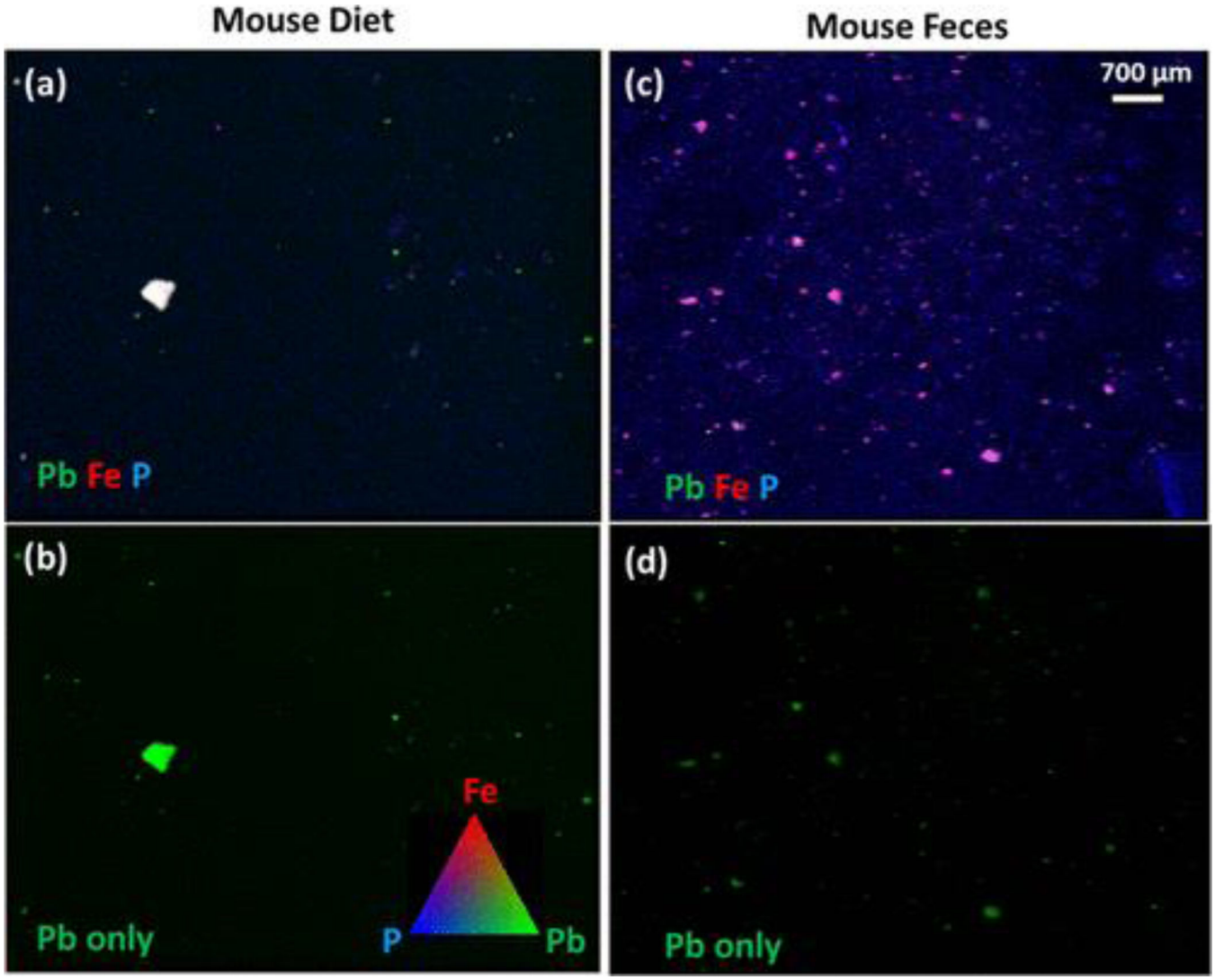

Figure 4.
µ-XRF localization of Pb, Fe, and P in diet and feces from mice that consumed diet amended with treated BHK5 soil.

EPA Author Manuscript

EPA Author Manuscript

EPA Author Manuscript

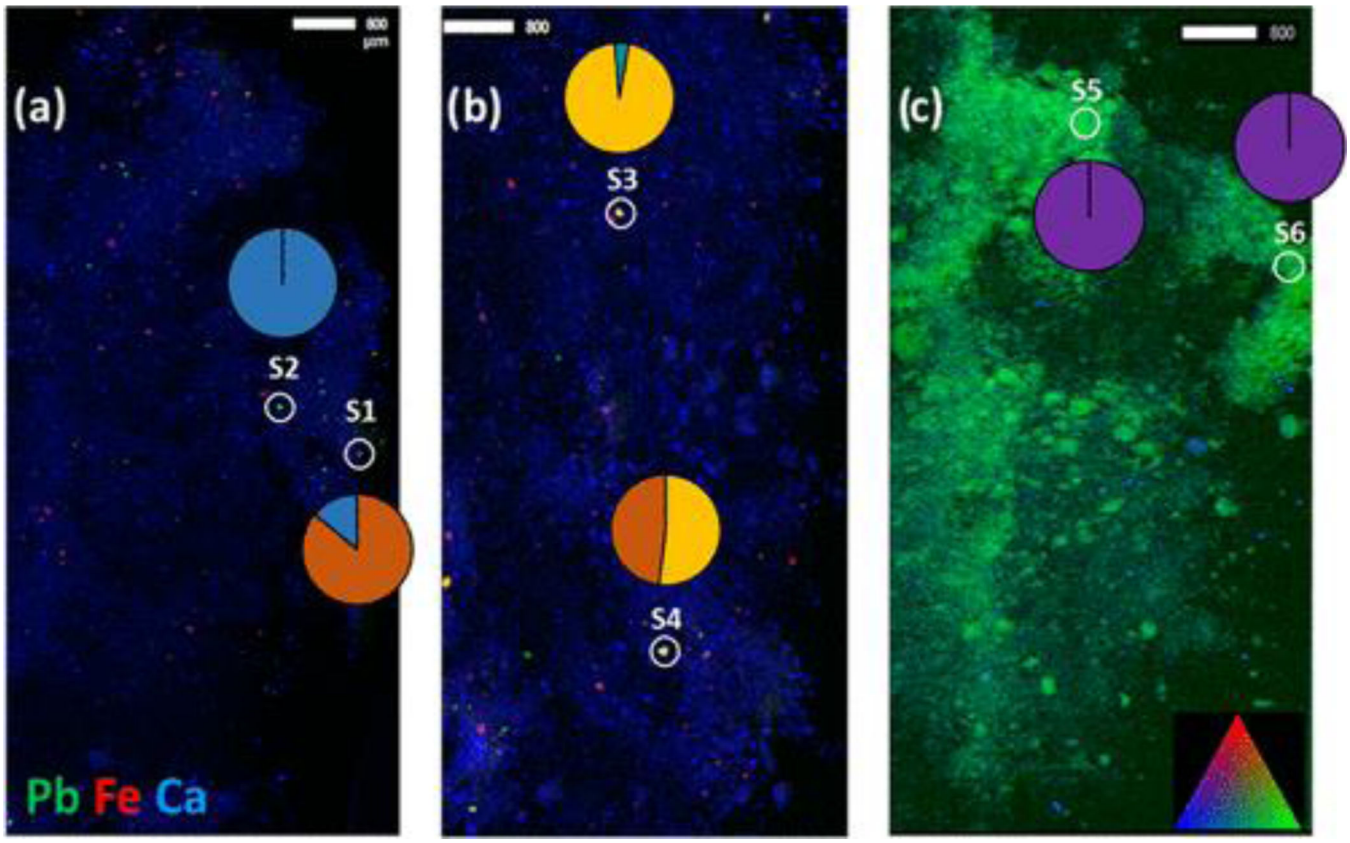

Figure 5.

µ-XRF cecal contents maps (scale bar in micrometers) for mice fed (a) BHK5-untreated, (b) BHK5-treated, or (c) Pb-acetate. Elemental maps are overlayed for Pb (green), Fe (red), and Ca (blue). Circled regions correspond to areas of spatially resolved Pb XANES analysis, where fitting results are shown in the pie charts for each area analyzed. Pb adsorbed to Fe oxide (brown box solid), hydroxyapatite (blue box solid), plumbojarosite (yellow box solid), anglesite (green box solid), and Pb acetate (purple box solid).

EPA Author Manuscript

EPA Author Manuscript

EPA Author Manuscript

Table 1.

Effect of Soil Treatment on Relative Bioavailability of Lead (Pb) in the Mouse[a]

soil	status	RBA	95 LCL	95 UCL	SE
BHK5	untreated	38.6	29.2	53.7	5.2
	treated	0.4	–0.6	1.5	0.4
BHK10	untreated	42.1	33.3	55.0	4.6
	treated	0.8	0.0	1.9	0.4

[a]Both Pb-contaminated soils originate from Broken Hill, Australia (BHK). Pb acetate RBA is assumed to be 100%. Percentage relative bioavailability (RBA) shown with estimated a 95% lower confidence limit (95 LCL), a 95% upper confidence limit (95 UCL), and % standard error (SE).